

Generalized $PP + PS = SS$ from seismic interferometry

David Halliday,¹ Andrew Curtis² and Kees Wapenaar³

¹Schlumberger Cambridge Research, High Cross, Madingley Road, Cambridge, CB3 0EL, UK. E-mail: dhalliday@slb.com

²School of GeoSciences, Grant Institute, The University of Edinburgh, Kings Buildings, West Mains Road, Edinburgh EH9 3JW, UK

³Department of Geoscience and Engineering, Delft University of Technology, PO Box 5048, 2600 GA Delft, The Netherlands

Accepted 2012 January 20. Received 2012 January 20; in original form 2011 August 31

SUMMARY

$PP + PS = SS$ refers to a method introduced by Grechka and Tsvankin in 2002 that uses recordings of PP and PS reflections between sources and receivers to estimate the SS reflections between those same receivers. Using source–receiver seismic interferometry as a basis, we derive new, dynamically correct expressions relating reflected and converted P - and S -wave recordings to both P - and S -wave sources. We use these expressions to derive a generalized form of relationship between P and S waves, and show that the $PP + PS = SS$ method of Grechka and co-workers is a special case of these new relationships. By considering the simple example of two elastic half-spaces, we illustrate the differences between the special case of $PP + PS = SS$ and the generalized approach derived here. By relating the method to seismic interferometry, it is possible to see further applications of the new relationships in acquisition and processing of P and S waves, and also in the development of new imaging and inversion schemes.

Key words: Interferometry; Controlled source seismology; Body waves; Theoretical seismology.

INTRODUCTION

The shear wave component of the seismic wavefield is important in determining the shear wave velocities in any medium. For example, in the Earth's subsurface the combination of P - and S -wave information allows fluid and rock properties to be discriminated. It is also particularly important in the study of anisotropic media where the polarizations of fast and slow split S waves are often used to infer the average alignment of fracture fields, or of crystalline lattice structures such as in uppermost mantle olivine.

In industrial geophysics, typically converted PS responses (P waves propagating down to a reflector at which the wave reflects and converts to S energy that propagates back to the surface) are used to infer S -wave velocity structure. However, this is undesirable from several points of view: both P - and S -wave velocity models are required to estimate reflection and conversion points, and Grechka & Tsvankin (2002) discuss the difficulty of velocity analysis for converted S waves due to the asymmetric moveout of the PS response. Ideally, pure PP responses (i.e. P -wave source, P -wave receiver) and pure SS responses (S -wave source, S -wave receiver) would be analysed independently.

Typically, the horizontal components of a three-component geophone are assumed to predominantly contain S waves whereas the vertical component is assumed to contain P waves. There are also various separation techniques that can be used to make more accurate measurements of the recorded P - and S -wavefields. For example, Curtis & Robertsson (2002) and Robertsson & Curtis (2002) introduce methods to separate P - and S -wave recordings using distributed arrays of three-component geophones. Sources of P -wave energy are also available as standard industrial equipment. However, it is far more difficult to inject significant S -wave energy into the ground economically.

Grechka & Tsvankin (2002) and Grechka & Dewangan (2003) proposed a potential solution to this problem: by combining PP and PS responses, pseudo-shear wave data can be generated that has the same kinematics as a pure SS response. Presumably, as the interest in elastic full waveform imaging and inversion grows, the recovery of shear wave velocity profiles, and the study of anisotropic media will come under greater scrutiny. Therefore, it is important to consider approaches such as that presented by Grechka & Tsvankin (2002) and Grechka & Dewangan (2003).

We examine the relationship between P - and S -wave energy in a novel way using theory from the field of seismic interferometry. Generally, seismic interferometry refers to the process of generating responses to imagined or virtual approximately impulsive sources by cross-correlation (Wapenaar 2003; van Manen *et al.* 2006; Wapenaar & Fokkema 2006), cross-convolution (e.g. Slob *et al.* 2007) or deconvolution (e.g. Vasconcelos & Snieder 2008a,b; Wapenaar *et al.* 2008, 2011) of wavefields from surrounding energy sources recorded at different receiver locations. Recent work has shown that intersource wavefields can be estimated by cross-correlating recordings of a pair of sources at a range of azimuths (Hong & Menke 2006; Curtis *et al.* 2009). Furthermore, Curtis & Halliday (2010) demonstrated that it is possible

to use so-called source–receiver interferometry to estimate the wavefield between a source and a receiver, allowing interferometry to be used to construct wavefields between any combination of source and receiver pairs. Halliday & Curtis (2010) also showed that the source–receiver relationships establish a direct link between seismic interferometry and seismic imaging. These theorems are generalized forms of existing imaging methods, for example, the methods of Oristaglio (1989) and Vasconcelos *et al.* (2010). Most generally, interferometry can be thought of as a method to synthesize desired wavefields that were not directly recorded. An example of such a wavefield is the *SS* response described earlier.

In this paper, we extend the applicability of the new source–receiver relationships by using the results of Curtis & Halliday (2010) to find interferometric relationships that describe precisely how *P*- and *S*-wave responses between sources and receivers are related. Wapenaar & Fokkema (2006) have already shown how *P*- and *S*-wave source and receivers can be incorporated within the framework for interferometry provided by reciprocity theorems of the correlation type, and the derivation in this paper follows a similar path to theirs. As a result, we derive the $PP + PS = SS$ equation of Grechka & Dewangan (2003) from source–receiver interferometry. Although the derivation of Grechka & Dewangan (2003) was in part heuristic and was purely kinematic, here we show that this can also be derived from first principles. The source–receiver representations that we consider are derived dynamically, directly from reciprocity and representation theorems (Curtis & Halliday 2010). This approach reveals the key approximations and assumptions inherent in the approach of Grechka & Tsvankin (2002) and Grechka & Dewangan (2003), and provides a theoretical framework to develop future *P*- and *S*-wave processing, imaging and inversion algorithms, potentially using novel combinations of *P*- and *S*-wave energy sources and receivers.

At the time of writing, there are already a range of applications that apply the single integral (virtual-source or virtual-receiver) forms of seismic interferometry using *P* and *S* waves. For example, Gaiser & Vasconcelos (2010) apply interferometry to seabed data to recover *PP*, *PS* and (potentially) *SS* responses, Bakulin & Mateeva (2008) apply seismic interferometry to horizontal component borehole geophones to create virtual-shear wave check shots, Miyazawa *et al.* (2008) apply seismic interferometry to ambient noise recorded in a borehole and show that they can observe shear wave splitting on the resultant virtual-source records, and van der Neut *et al.* (2011) outline a theoretical framework for the application of multidimensional deconvolution using separated *P* and *S* waves. Tonegawa & Nishida (2010) study earthquake records and show that virtual-receiver seismic interferometry (Curtis *et al.* 2009) can be used to recover direct *P* and *S* waves propagating between pairs of deep earthquakes. While an application of the (double-integral) form of source–receiver interferometry that differentiates *P* and *S* waves has yet to be published, here we will demonstrate that the $PP + PS = SS$ method may be considered as such an application. Moreover, the relationships derived here provide a framework for the development of future applications of source–receiver interferometry using *P*- and *S*-wave sources and receivers.

First, we consider the derivation of source–receiver interferometric relationships for *P*- and *S*-wave sources and receivers. We illustrate that in the general case, with a source and receiver located within two enclosing boundaries, the recovery of the *SS* reflection response through interferometry alone (i.e. without recording it directly) in a simple example requires only *S*-wave sources and *S*-wave receivers. Then, we introduce the approximations and assumptions required to derive the special case of $PP + PS = SS$ published by Grechka & Dewangan (2003). In this special case, contrary to the general case, no *S*-wave sources are required. Using the same simple model, we illustrate the key differences between the $PP + PS = SS$ approach, and this general approach based on the new representations derived here. Finally, we discuss further applications of the source–receiver integrals for *P* and *S* waves.

SOURCE–RECEIVER REPRESENTATION FOR *P* AND *S* WAVES

We now derive the source–receiver representations for *P* and *S* waves by following the approach of Curtis & Halliday (2010, appendix A). In the following, we will also take advantage of the *P*- and *S*-wave Green's functions used by Wapenaar & Haimé (1990) and Wapenaar & Fokkema (2006).

Using the elastodynamic representation theorem, Curtis & Halliday (2010, appendix A) show that the response between a real source and a real receiver in a lossless inhomogeneous anisotropic medium can be derived using two correlation-type representation theorems.

$$G_{qm}(\mathbf{x}_2, \mathbf{x}_1) - G_{qm}^*(\mathbf{x}_2, \mathbf{x}_1) = \int_S \{ G_{qn}^*(\mathbf{x}_2, \mathbf{x}) n_j c_{njkl} \partial_k \Phi_{ml}(\mathbf{x}_1, \mathbf{x}) - n_j c_{njkl} \partial_k G_{ql}^*(\mathbf{x}_2, \mathbf{x}) \Phi_{mn}(\mathbf{x}_1, \mathbf{x}) \} dS, \quad (1)$$

where

$$\Phi_{ml}(\mathbf{x}_1, \mathbf{x}) = - \int_{S'} \{ G_{n'l}(\mathbf{x}', \mathbf{x}) n_{j'} c_{n'j'k'l'} \partial_{k'} G_{l'm}^*(\mathbf{x}', \mathbf{x}_1) - n_{j'} c_{n'j'k'l'} \partial_{k'} G_{l'l'}(\mathbf{x}', \mathbf{x}) G_{n'm}^*(\mathbf{x}', \mathbf{x}_1) \} dS'. \quad (2)$$

Here, $G_{qm}(\mathbf{x}_2, \mathbf{x}_1)$ is the Green's function in the frequency domain representing the q th component of particle displacement at \mathbf{x}_2 due to a unidirectional point force in the m -direction at \mathbf{x}_1 , n_j is the j th component of the normal vector on the boundary S , ∂_k denotes a spatial derivative in the k -direction and c_{njkl} is the stiffness tensor. Primed and unprimed quantities indicate that these relate to the primed and unprimed boundaries, respectively (Fig. 1a), and Einstein's summation principle for repeated indices applies throughout.

Eq. (1) describes the recovery of a Green's function (plus its time reverse due to the complex conjugate on the left-hand side) between a source at \mathbf{x}_1 and a receiver at \mathbf{x}_2 in elastic media, using only Green's functions from \mathbf{x}_1 to a surrounding boundary S' of receivers, and Green's functions from a surrounding boundary S (Fig. 1a). The integral in eq. (2) describes a first step where the boundary S' is used to determine the Green's functions (plus the time reverse) between the source at \mathbf{x}_1 and each source on the boundary S ; hence, this first step turns the source \mathbf{x}_1 into a virtual receiver. In a second step, the boundary S is used to determine the Green's function between the receiver at \mathbf{x}_2 and

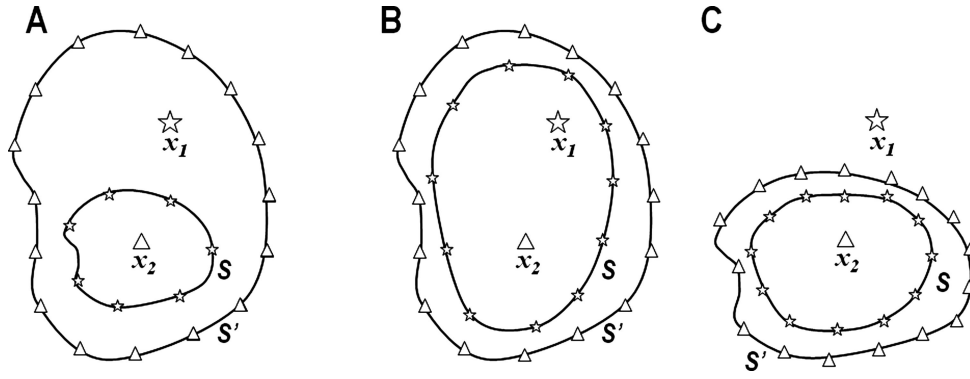


Figure 1. Canonical geometries for source–receiver interferometry for (a) the correlation–correlation, (b) the correlation–convolution, and (c) the convolution–convolution forms (Curtis & Halliday 2010). Note the different positions of \mathbf{x}_1 and \mathbf{x}_2 relative to the boundaries.

the newly generated virtual receiver \mathbf{x}_1 (in reality, a source). Thus, this interferometric integral uses both surrounding sources and receivers to reconstruct virtual-source to virtual-receiver wavefields. This specific form of the integral is derived by combining two representation theorems of the correlation type and can be used in the canonical geometry represented in Fig. 1(a) where the source and receiver both lie within both boundaries. Figs 1(b) and (c) show other configurations that can be derived using (b) both correlation- and convolution-type representation theorems, and (c) two convolution-type representation theorems, respectively (Curtis & Halliday 2010).

To extend eq. (1) to describe the recovery of P and S responses, we recall from Wapenaar & Fokkema (2006) that the P - and S -wave components of the wavefield can be expressed as a sum of partial derivatives of the displacement

$$G_{\psi_{0m}}(\mathbf{x}_2, \mathbf{x}_1) = -\rho c_p^2 \partial_q G_{qm}(\mathbf{x}_2, \mathbf{x}_1), \quad (3)$$

$$G_{\psi_{km}}(\mathbf{x}_2, \mathbf{x}_1) = \rho c_s^2 \varepsilon_{kjq} \partial_j G_{qm}(\mathbf{x}_2, \mathbf{x}_1), \quad (4)$$

where c_s is the local S -wave velocity at \mathbf{x}_2 , c_p is the local P -wave velocity at \mathbf{x}_2 , ρ is the density at \mathbf{x}_2 , ω is the angular frequency, $G_{\psi_{km}}(\mathbf{x}_2, \mathbf{x}_1)$ is the Green's function representing the S wave at \mathbf{x}_2 polarized in the plane with normal \mathbf{n}_k , due to a point force in the m -direction at \mathbf{x}_1 and $G_{\psi_{0m}}(\mathbf{x}_2, \mathbf{x}_1)$ is the equivalent Green's function for a P wave at \mathbf{x}_2 . ε_{kij} is the alternating tensor with $\varepsilon_{123} = \varepsilon_{312} = \varepsilon_{231} = -\varepsilon_{213} = -\varepsilon_{321} = -\varepsilon_{132} = 1$. When we interpret eqs (3) and (4) as P - and S -wave Green's functions, we assume that the medium is homogeneous and isotropic locally around the receiver point, \mathbf{x}_2 . In the following, we will use one notation for the Green's function, $G_{\psi_{Km}}(\mathbf{x}_2, \mathbf{x}_1)$, with K equal to 0, 1, 2 or 3. $K = 0$ denotes P waves (*cf.* eq. 3) and $K = 1, 2$ or 3 denotes a shear wave polarized in the plane with normal \mathbf{n}_K (*cf.* eq. 4), assuming appropriate P or S velocities are used.

Eqs (3) and (4) are weighted sums of the spatial derivatives of point-force responses (and likewise, by reciprocity, we can find similar expressions for the particle displacement due to P - and S -wave sources—see Wapenaar & Fokkema (2006)). Hence, eqs (3) and (4) show how appropriately weighted sums of partial derivatives of eq. (1) represent P - and S -wave source and receiver Green's functions. Evaluating these sums explicitly using eq. (1) results in

$$G_{\psi_Q \psi_M}(\mathbf{x}_2, \mathbf{x}_1) - G_{\psi_Q \psi_M}^*(\mathbf{x}_2, \mathbf{x}_1) = \int_S \left\{ G_{\psi_Q n}^*(\mathbf{x}_2, \mathbf{x}) n_j c_{njkl} \partial_k \Psi_{\psi_M l}(\mathbf{x}_1, \mathbf{x}) - n_j c_{njkl} \partial_k G_{\psi_Q l}^*(\mathbf{x}_2, \mathbf{x}) \Psi_{\psi_M n}(\mathbf{x}_1, \mathbf{x}) \right\} dS, \quad (5)$$

with

$$\Psi_{\psi_M l}(\mathbf{x}_1, \mathbf{x}) = - \int_{S'} \left\{ G_{n' l}(\mathbf{x}', \mathbf{x}) n_{j'} c_{n' j' k' l'} \partial_{k'} G_{l' \psi_M}^*(\mathbf{x}', \mathbf{x}_1) - n_{j'} c_{n' j' k' l'} \partial_{k'} G_{l' l}(\mathbf{x}', \mathbf{x}) G_{n' \psi_M}^*(\mathbf{x}', \mathbf{x}_1) \right\} dS'. \quad (6)$$

Here, $G_{\psi_Q \psi_M}(\mathbf{x}_2, \mathbf{x}_1)$ is the Green's function representing the P - or S -wave component of the wavefield at \mathbf{x}_2 due to a P - or S -wave source at \mathbf{x}_1 . $G_{n' \psi_M}(\mathbf{x}', \mathbf{x}_1)$ is the Green's function representing the n' th component of particle displacement at \mathbf{x}' due to a P - or S -wave source at \mathbf{x}_1 . On the source component, the uppercase subscript M runs from 0 to 3, with 0 denoting a P -wave source, and 1 to 3 denoting a shear wave source polarized in the plane with normal \mathbf{n}_M .

While the left-hand side of eq. (5) now contains only P -to- S , S -to- P , P -to- P or S -to- S Green's functions, the right-hand side of eq. (5) and also eq. (6) contain Green's functions that require particle displacement and unidirectional point forces on the surfaces S' and S , respectively. We now follow Wapenaar & Fokkema (2006) in changing these to be P - and S -wave receivers or sources. First, we consider the integral in eq. (6): from Wapenaar & Fokkema (2006, equations 72 and 73) we can write

$$\Psi_{\psi_M l}(\mathbf{x}_1, \mathbf{x}) = - \frac{2}{\rho} \int_{S'} \partial_{j'} G_{\psi_K l}(\mathbf{x}', \mathbf{x}) G_{\psi_K \psi_M}^*(\mathbf{x}', \mathbf{x}_1) dS'. \quad (7)$$

Because we use P - and S -wave quantities on the boundary, we are assuming that the medium at and outside the boundary S' is homogeneous and isotropic. Applying the same principles to the integral over S such that it consists of only recordings of P - and S -wave sources, we obtain

$$G_{\psi_Q \psi_M}(\mathbf{x}_2, \mathbf{x}_1) - G_{\psi_Q \psi_M}^*(\mathbf{x}_2, \mathbf{x}_1) = \frac{4}{\rho^2} \int_S \int_{S'} \partial_j G_{\psi_Q \psi_K}^*(\mathbf{x}_2, \mathbf{x}) \partial_{j'} G_{\psi_K \psi_M}(\mathbf{x}', \mathbf{x}) G_{\psi_K \psi_M}^*(\mathbf{x}', \mathbf{x}_1) n_{j'} n_j dS' dS. \quad (8)$$

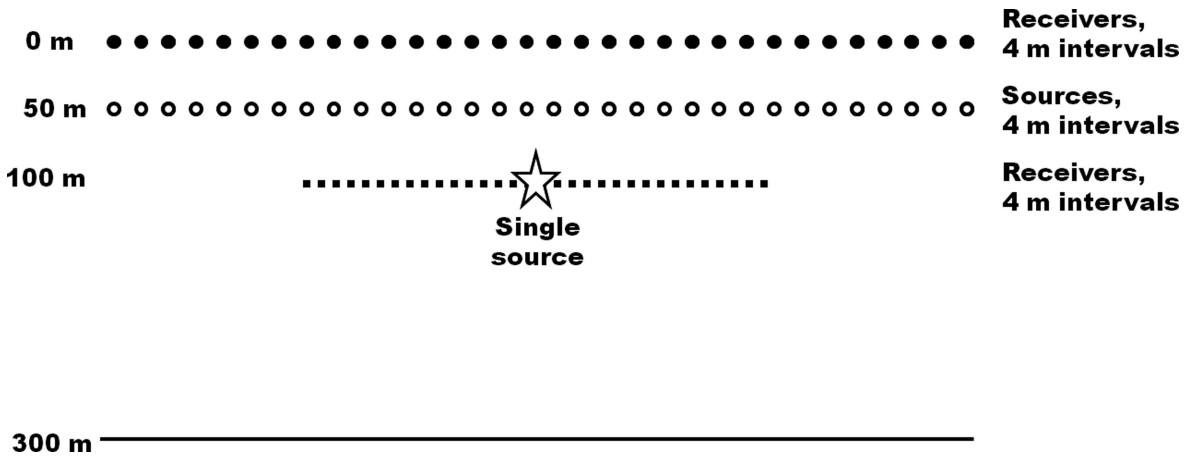


Figure 2. Sketch of the setup used to calculate the finite difference synthetic data. Black filled circles represent the line of receivers used as the boundary S' , white filled circles represent the line of sources used as the boundary S , the star indicates the single source, \mathbf{x}_1 , and the black dotted line represents the receivers \mathbf{x}_2 at which we wish to reconstruct the response due to the source at \mathbf{x}_1 . The solid black line indicates the single reflector.

Again, we assume that the medium at and outside the boundary S is isotropic and homogeneous. Eq. (8) is a generalized form of the $PP + PS = SS$ equation used by Grechka & Dewangan (2003). This describes the recovery of any combination of P - and S -wave source and receiver from other P - and S -wave sources and receivers. We can also split the right-hand side into integrals dependent on PP ($\psi_K = \psi_0, \psi'_K = \psi'_0$), PS ($\psi_K = \psi_0, \psi'_K = \psi'_k$), SP ($\psi_K = \psi_k, \psi'_K = \psi'_0$) and SS responses ($\psi_K = \psi_k, \psi'_K = \psi'_k$). Thus, if we wish to recover the SS response ($\psi_Q = \psi_q, \psi_M = \psi_m$) for example, we can write

$$\begin{aligned}
 G_{\psi_q \psi_m}(\mathbf{x}_2, \mathbf{x}_1) - G_{\psi_q \psi_m}^*(\mathbf{x}_2, \mathbf{x}_1) &= \frac{4}{\rho^2} \int_S \int_{S'} \partial_j G_{\psi_q \psi_0}^*(\mathbf{x}_2, \mathbf{x}) \partial_{j'} G_{\psi'_k \psi_0}(\mathbf{x}', \mathbf{x}) G_{\psi'_k \psi_m}^*(\mathbf{x}', \mathbf{x}_1) n_{j'} n_j dS' dS \\
 &+ \frac{4}{\rho^2} \int_S \int_{S'} \partial_j G_{\psi_q \psi_k}^*(\mathbf{x}_2, \mathbf{x}) \partial_{j'} G_{\psi'_0 \psi_k}(\mathbf{x}', \mathbf{x}) G_{\psi'_0 \psi_m}^*(\mathbf{x}', \mathbf{x}_1) n_{j'} n_j dS' dS \\
 &+ \frac{4}{\rho^2} \int_S \int_{S'} \partial_j G_{\psi_q \psi_k}^*(\mathbf{x}_2, \mathbf{x}) \partial_{j'} G_{\psi'_k \psi_k}(\mathbf{x}', \mathbf{x}) G_{\psi'_k \psi_m}^*(\mathbf{x}', \mathbf{x}_1) n_{j'} n_j dS' dS \\
 &+ \frac{4}{\rho^2} \int_S \int_{S'} \partial_j G_{\psi_q \psi_0}^*(\mathbf{x}_2, \mathbf{x}) \partial_{j'} G_{\psi'_0 \psi_0}(\mathbf{x}', \mathbf{x}) G_{\psi'_0 \psi_m}^*(\mathbf{x}', \mathbf{x}_1) n_{j'} n_j dS' dS.
 \end{aligned} \tag{9}$$

Similar expressions can be written for any other type of response on the left-hand side of eq. (9). For illustration, consider the simple example of two elastic half-spaces (Fig. 2). As in the $PP + PS = SS$ method, the aim of this example is to recover the SS reflection response between a source and a receiver using other types of responses from and to that source and receiver, respectively. In the following, we make some assumptions based on the stationary phase approach for reflected waves discussed by Snieder *et al.* (2006). First, because we are interested only in the reflected waves, and we assume that transmitted waves from sources on the lower boundary do not contribute to this, we set the contribution from this part of the boundary to be equal to zero. Lines extending to infinity are then used in place of closed surfaces S and S' . Secondly, we assume that the source-to-receiver singly reflected wave will result from the direct waves between each source on the boundary S and the receiver at \mathbf{x}_2 , the direct waves between the source at \mathbf{x}_1 and each receiver on the boundary S' and the reflected waves between each source on S and each receiver on S' . This means that the PS and SP responses between \mathbf{x}_2 and \mathbf{x} , and \mathbf{x} and \mathbf{x}_1 are equal to zero, since the direct wave is not subject to any P -to- S or S -to- P conversions. Thus, the first, second and fourth integrals on the right-hand side of eq. (9) are equal to zero, and we consider application of the following resulting equation:

$$G_{\psi_q \psi_m}^r(\mathbf{x}_2, \mathbf{x}_1) - G_{\psi_q \psi_m}^{d*}(\mathbf{x}_2, \mathbf{x}_1) = \frac{4}{\rho^2} \int_S \int_{S'} \partial_j G_{\psi_q \psi_k}^{d*}(\mathbf{x}_2, \mathbf{x}) \partial_{j'} G_{\psi'_k \psi_k}^r(\mathbf{x}', \mathbf{x}) G_{\psi'_k \psi_m}^{d*}(\mathbf{x}', \mathbf{x}_1) n_{j'} n_j dS' dS, \tag{10}$$

where the superscripts r and d indicate reflected waves and direct waves, respectively. Eq. (10) shows how the SS response between \mathbf{x}_1 and \mathbf{x}_2 can be constructed using only the responses from S -wave sources recorded on S -wave receivers.

Fig. 2 shows a sketch of the example considered here. We will use both simple sketches and finite difference synthetic seismograms (Robertsson *et al.* 1994) to illustrate the example. A single reflector exists at 300 m depth, there is a horizontal line of 250 receivers separated at 4 m intervals at 0 m depth, a horizontal line of 250 sources separated at 4 m intervals at 50 m depth, a line of 100 receivers separated at 4 m intervals at 100 m depth and a single source centred on that line. The top half-space has a P -wave velocity of 1500 m s⁻¹, an S -wave velocity of 800 m s⁻¹ and a density of 1700 kg m⁻³. Corresponding parameters for the bottom half-space are 2400 m s⁻¹, 1000 m s⁻¹ and 2000 kg m⁻³, respectively. The medium is lossless. The aim of the example is to estimate the SS reflections between the source at 100 m depth and each receiver on the line at the same depth. To allow accurate separation of direct and reflected waves, each synthetic seismogram is modelled twice, once without the reflector to give the direct wave only, and once with the reflector to give the direct wave and the reflected wave. The reflected wave is then separated by taking the difference of the two.

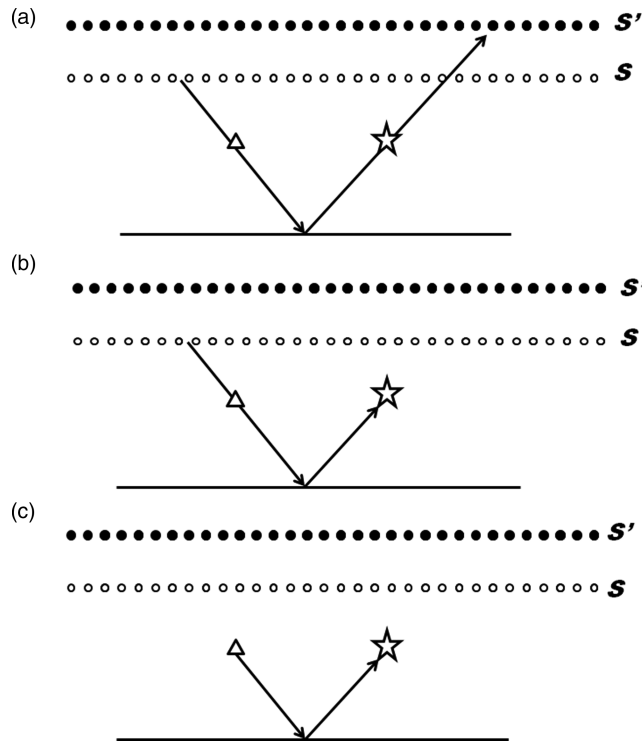


Figure 3. Sketch example of the kinematics involved in recovering the SS reflection using eq. (10). White circles indicate a line of sources, black circles indicate a line of receivers, the triangle is a single receiver and the star is a single source. (a) The starting point is the SS reflection between each source on the boundary S , and each receiver on the boundary S' . (b) The first step is the cross-correlation of the interboundary responses with the direct S wave between the single source and boundary of receivers. The result is the SS reflection between the boundary of sources, and the single source. (c) The second step is cross-correlation of the intersource SS reflections with the direct S wave between the source boundary and the single receiver. This results in the SS reflection between the source and receiver.

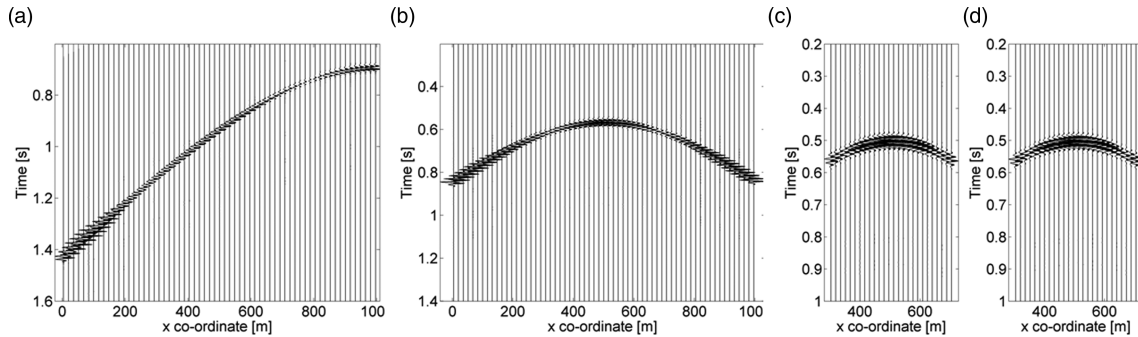


Figure 4. (a) SS response between a source on the boundary and the boundary of receivers illustrated in Fig. 3(a). (b) The result of the first cross-correlation step which gives the SS reflection between the source boundary and the single source (Fig. 3b). (c) The result of using source–receiver interferometry to recover the SS reflection (Fig. 3c) and (d) the directly modelled SS reflection (accounting for the scale factor introduced in the interferometric estimates).

Fig. 3 shows a number of sketches that illustrate the construction of the unmeasured SS response using eq. (10). Fig. 3(a) shows a sketch of the SS response between a boundary source (white circles), and a boundary receiver (black filled circles). The first pass of interferometry (i.e. solution of the integral over S' in eq. 10) uses the direct S wave from the boundary of receivers to compute the SS reflection between the boundary of sources and the single source (star). Fig. 3(b) shows this intermediate step, where the part of the ray path between the boundary of receivers and the single source has been removed (*cf.* Fig. 3a). The second pass of interferometry (i.e. solution of the integral over S) uses the direct S wave from the boundary of sources to the single receiver (triangle) to compute the SS reflection between the single receiver and the source. Fig. 3(c) shows the equivalent sketch, where the part of the ray path between the boundary of sources and the single receiver has been removed, resulting in the reflected wave between the source and the receiver.

Figs 4(a)–(c) show the synthetic data corresponding to the illustrations in Figs 3(a)–(c). These are (a) the SS reflection response between a single boundary source and each boundary receiver, (b) the intermediate SS reflection response between each boundary source, and the single source, (c) the SS reflection response between a source and a line of receivers resulting from eq. (10) and (d) the directly modelled SS reflection response for comparison (right-hand panel). A scale factor is required for the amplitude and phase of panels (c) and (d) to match (the scale factor is due to the source wavelet and implementation of the source function used in the finite difference code). With the application

of this scale factor it is difficult to see any difference between the directly modelled source gather, and the source gather constructed with source-receiver interferometry. This validates both the approach used to derive eq. (9), and also the assumptions based on stationary phase used to reach eq. (10).

Thus, in the configuration sketched in Fig. 1(a) we see that the *SS* response is constructed without the use of any *P*-wave component (either at the source or the receiver). This is contrary to the approach of Grechka & Tsvankin (2002) and Grechka & Dewangan (2003) who require both a *P*-wave source and a *P*-wave receiver. In the next section, we will illustrate the special conditions under which their method can be applied.

PP + PS = SS

We now show that the approach of Grechka & Dewangan (2003, eq. 5) to recover *SS* reflection responses from conventional (*P*-wave source) seismic data can be considered a special case of eq. (8). Rather than constructing the *SS* reflection response using only *S*-wave sources and *S*-waves receivers, Grechka and Dewangan do not use *S*-wave sources as an input. We move all the terms dependent on *SS* responses to the left-hand side of eq. (9)

$$\begin{aligned} G_{\psi_q \psi_m}(\mathbf{x}_2, \mathbf{x}_1) - G_{\psi_q \psi_m}^*(\mathbf{x}_2, \mathbf{x}_1) &- \frac{4}{\rho^2} \int_S \int_{S'} \partial_j G_{\psi_q \psi_0}^*(\mathbf{x}_2, \mathbf{x}) \partial_{j'} G_{\psi'_k \psi_0}(\mathbf{x}', \mathbf{x}) G_{\psi'_k \psi_m}^*(\mathbf{x}', \mathbf{x}_1) n_{j'} n_j dS' dS \\ &- \frac{4}{\rho^2} \int_S \int_{S'} \partial_j G_{\psi_q \psi_k}^*(\mathbf{x}_2, \mathbf{x}) \partial_{j'} G_{\psi'_0 \psi_k}(\mathbf{x}', \mathbf{x}) G_{\psi'_0 \psi_m}^*(\mathbf{x}', \mathbf{x}_1) n_{j'} n_j dS' dS \\ &- \frac{4}{\rho^2} \int_S \int_{S'} \partial_j G_{\psi_q \psi_k}(\mathbf{x}_2, \mathbf{x}) \partial_{j'} G_{\psi'_k \psi_k}(\mathbf{x}', \mathbf{x}) G_{\psi'_k \psi_m}^*(\mathbf{x}', \mathbf{x}_1) n_{j'} n_j dS' dS \\ &= \frac{4}{\rho^2} \int_S \int_{S'} \partial_j G_{\psi_q \psi_0}(\mathbf{x}_2, \mathbf{x}) \partial_{j'} G_{\psi'_0 \psi_0}(\mathbf{x}', \mathbf{x}) G_{\psi'_0 \psi_m}^*(\mathbf{x}', \mathbf{x}_1) n_{j'} n_j dS' dS. \end{aligned} \quad (11)$$

Since Grechka & Dewangan (2003) consider only *PP* and *PS* responses, we group all other responses together and define these as

$$\begin{aligned} Z_{\psi_q \psi_m}(\mathbf{x}_2, \mathbf{x}_1) &= -\frac{4}{\rho^2} \int_S \int_{S'} \partial_j G_{\psi_q \psi_0}^*(\mathbf{x}_2, \mathbf{x}) \partial_{j'} G_{\psi'_k \psi_0}(\mathbf{x}', \mathbf{x}) G_{\psi'_k \psi_m}^*(\mathbf{x}', \mathbf{x}_1) n_{j'} n_j dS' dS \\ &- \frac{4}{\rho^2} \int_S \int_{S'} \partial_j G_{\psi_q \psi_k}^*(\mathbf{x}_2, \mathbf{x}) \partial_{j'} G_{\psi'_0 \psi_k}(\mathbf{x}', \mathbf{x}) G_{\psi'_0 \psi_m}^*(\mathbf{x}', \mathbf{x}_1) n_{j'} n_j dS' dS \\ &- \frac{4}{\rho^2} \int_S \int_{S'} \partial_j G_{\psi_q \psi_k}(\mathbf{x}_2, \mathbf{x}) \partial_{j'} G_{\psi'_k \psi_k}(\mathbf{x}', \mathbf{x}) G_{\psi'_k \psi_m}^*(\mathbf{x}', \mathbf{x}_1) n_{j'} n_j dS' dS, \end{aligned} \quad (12)$$

where after eq. (11) is rewritten as

$$G_{\psi_q \psi_m}(\mathbf{x}_2, \mathbf{x}_1) - G_{\psi_q \psi_m}^*(\mathbf{x}_2, \mathbf{x}_1) + Z_{\psi_q \psi_m}(\mathbf{x}_2, \mathbf{x}_1) = \frac{4}{\rho^2} \int_S \int_{S'} \partial_j G_{\psi_q \psi_0}(\mathbf{x}_2, \mathbf{x}) \partial_{j'} G_{\psi'_0 \psi_0}(\mathbf{x}', \mathbf{x}) G_{\psi'_0 \psi_m}^*(\mathbf{x}', \mathbf{x}_1) n_{j'} n_j dS' dS. \quad (13)$$

If both boundaries *S'* and *S* are spheres with very large radius such that energy to (from) location \mathbf{x}_1 (\mathbf{x}_2) leaves (arrives) at the boundary approximately perpendicularly, then the spatial derivatives in eq. (13) can be approximated by, $\partial_j n_j = -j\omega/c_K$, where, $c_K = c_P$ for $K = 0$, and $c_K = c_S$ for $K = 1, 2$ or 3 . $Z_{\psi_q \psi_m}(\mathbf{x}_2, \mathbf{x}_1)$ includes terms that require *S*-wave sources, and in practice this type of seismic source is not usually available. We will therefore neglect the contributions due to this term. Eq. (13) can then be written as

$$G_{\psi_q \psi_m}(\mathbf{x}_2, \mathbf{x}_1) - G_{\psi_q \psi_m}^*(\mathbf{x}_2, \mathbf{x}_1) \approx \frac{4\omega^2}{c_P c_{P'} \rho^2} \int_S \int_{S'} G_{\psi_q \psi_0}^*(\mathbf{x}_2, \mathbf{x}) G_{\psi'_0 \psi_0}(\mathbf{x}', \mathbf{x}) G_{\psi'_0 \psi_m}^*(\mathbf{x}', \mathbf{x}_1) dS' dS. \quad (14)$$

Despite the fact that we have neglected the term dependent on *S*-wave sources, in the following the kinematics of the *SS* reflection response are recovered, even when the *S*-wave sources are not considered. Note also that the final term on the right-hand side ($G_{\psi'_0 \psi_m}^*(\mathbf{x}', \mathbf{x}_1)$) is the reflected *P* wave ($M = 0$) due to an *S*-wave source ($M = m$). Since no *S*-wave sources are used in this approach source–receiver reciprocity may be used such that this term is obtained from the reflected *S* wave due to a *P*-wave source $G_{\psi_m \psi'_0}(\mathbf{x}_1, \mathbf{x}')$. This requires that \mathbf{x}_1 is a receiver and \mathbf{x}' is both a source and a receiver. Hence, the boundary of sources and the boundary of receivers must be collocated, to allow both $G_{\psi_m \psi'_0}(\mathbf{x}_1, \mathbf{x}')$ and $G_{\psi'_0 \psi_0}(\mathbf{x}', \mathbf{x})$ to be measured. This introduces zero-offset Green's functions, but we can avoid associated complications by assuming that we are only interested in the reflected and/or scattered part of the wavefield. Using the notation of eq. (10), this gives

$$G_{\psi_q \psi_m}^r(\mathbf{x}_2, \mathbf{x}_1) - G_{\psi_q \psi_m}^{r*}(\mathbf{x}_2, \mathbf{x}_1) \approx \frac{4\omega^2}{c_P c_{P'} \rho^2} \int_S \int_{S'} G_{\psi_q \psi_0}^{r*}(\mathbf{x}_2, \mathbf{x}) G_{\psi'_0 \psi_0}^r(\mathbf{x}', \mathbf{x}) G_{\psi'_0 \psi_m}^{r*}(\mathbf{x}_1, \mathbf{x}') dS' dS. \quad (15)$$

We now consider the same two half-space example as above. To accommodate the application of eq. (15), we move all sources and receivers onto the same surface. In reaching eq. (15), we assumed that the source and receiver boundaries were collocated, and in the following example we illustrate that both \mathbf{x}_1 and \mathbf{x}_2 must also be located on this same surface for the relation *PP + PS = SS*. Thus, rather than having sources and receivers distributed across a range of depths as in Fig. 3(a), we now consider all sources and receivers at a depth of 0 m (Fig. 5a).

We again begin with a sketched example. Fig. 5(a) shows the ray path for a reflected *PP* wave between a source and receiver on the same boundary. We denote the phase of the downgoing *P* wave as *P1* and the phase of the upgoing *P* wave as *P2* (the phase of this reflection is then denoted as *P1 + P2*). In this example, the first step is cross-correlation of the *PP* wave with a *PS* reflection (*P1 + S2*). The result of

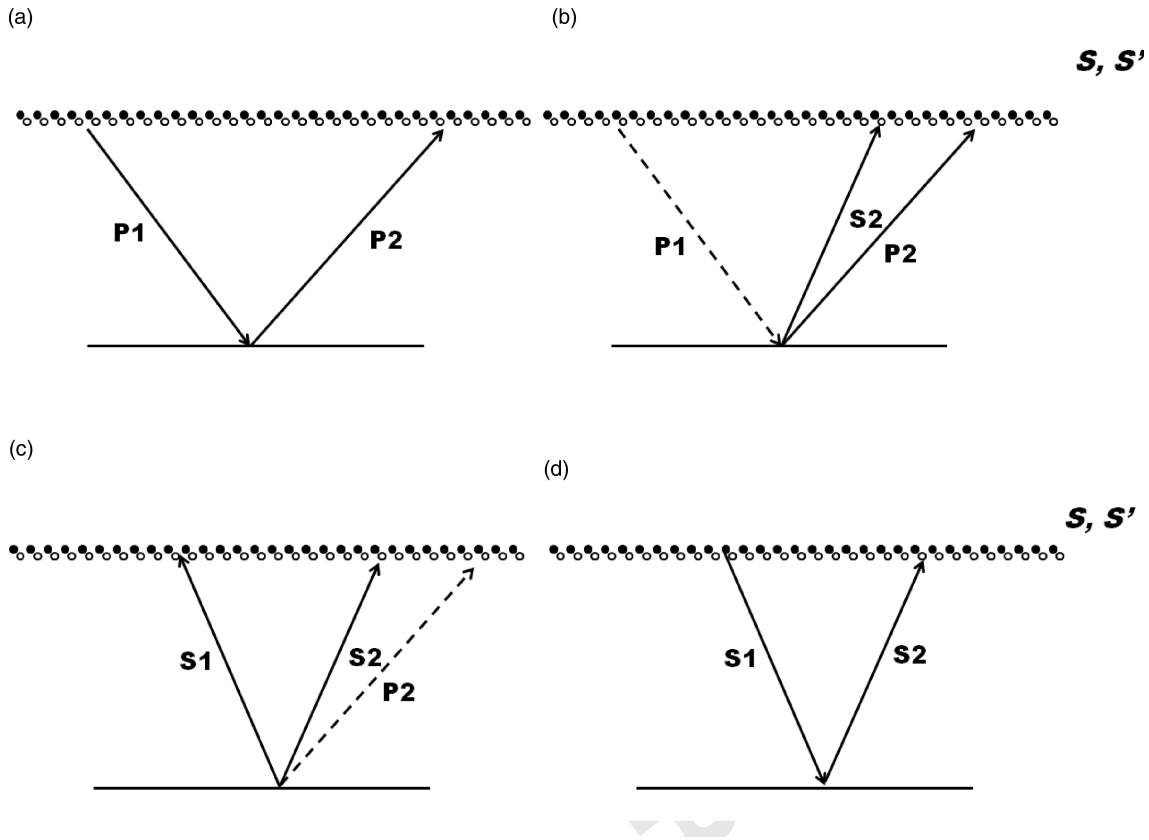


Figure 5. Sketch example of the kinematics involved in recovering the SS reflection using eq. (15). Black circles indicate a line of receivers and white circles indicate a line of sources. (a) The starting point is the PP reflection between each source on the boundary and each receiver on the boundary, $P1$ and $P2$ denote the phases of the downgoing and upgoing legs of the reflection, respectively. (b) For a chosen source and receiver pair on the boundary, the first step is the cross-correlation of the interboundary PP responses with the reflected PS ($P1 + S2$) wave. The dashed line indicates the common travel path ($P1$) removed by cross-correlation. The result is a non-physical event with a traveltime equivalent to the difference between the traveltime of the upward leg of the PS reflection ($S2$) and the upward leg of the PP reflection ($P2$). (c) The second step is cross-correlation of this intermediate event with the SP reflection ($S1 + P2$). The dash line again indicates the common travel path ($P2$) removed by cross-correlation. (d) The results is the (time reverse of the) SS reflection ($S1 + S2$).

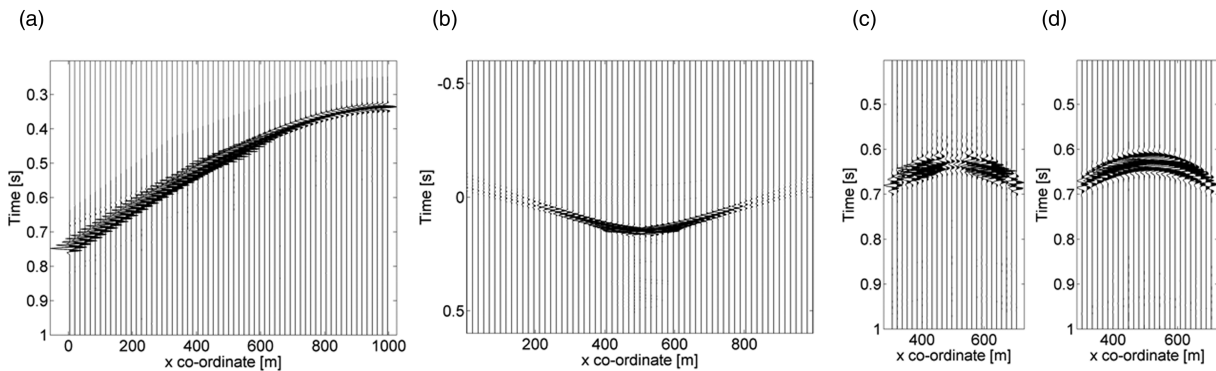


Figure 6. (a) PP response between a source on the boundary illustrated in Fig. 5 and the boundary of receivers. (b) The result of the first cross-correlation step which gives a non-physical arrival with a traveltime equivalent to the traveltime difference of the upward leg of a PS reflection and the upward leg of a PP reflection. (c) The result of the $PP + PS = SS$ method to recover the SS reflection and (d) the directly modelled SS reflection (accounting for scale factors introduced in the interferometric estimates).

this intermediate step is illustrated in Fig. 5(b). The cross-correlation removes the common path which is the downgoing P wave ($P1$). The phase of this intermediate step is then $P2 - S2$. The result of this intermediate step is cross-correlated with the P -to- S reflection travelling in the opposite direction (illustrated in Fig. 5c with phase $S1 + P2$). The common path is the upgoing P wave $P2$, and the result of this second correlation is $-(S1 + S2)$ and this results in the pseudo- SS reflection response—an event with the same traveltime as the SS reflected wave between a source and a receiver (in this case we have recovered the time-reverse of the SS reflection).

Fig. 6 shows the synthetic example corresponding to the illustrations in Fig. 5. These are: (a) the PP reflection response between a source and each receiver, (b) the intermediate result after the first PS cross-correlation (note the existence of causal and acausal parts; this

intermediate step is non-physical), (c) the pseudo-SS reflection response between a source and a line of receivers and (d) the directly modelled SS reflection response for comparison (right-hand panel). Note that as in Fig. 4(c), the traveltimes are correctly recovered using this method, but there are differences in amplitudes of the estimated response and directly computed response. In this case, these cannot be removed by applying a single-scale factor, because they are caused by neglecting the (dynamically varying) terms with S -wave sources to reach eq. (14).

Thus, in this second configuration sketched in Fig. 5, the SS reflection response is constructed without the use of any S -wave source components. This special case is different to the general case in which S sources are required to construct the SS responses, and it requires that both source and receiver boundaries are collocated, and that the particular source and receiver between which the Green's function is to be constructed also lie on the same source/receiver boundary.

Note that we have considered the result of two cross-correlations to recover the SS response. This is consistent with eq. (15) which contains two complex conjugations. However, Grechka & Dewangan (2003) show that the SS response can be recovered from the result of a cross-correlation and a convolution. If we take the complex conjugate of both sides of eq. (15), we find

$$G_{\psi_q \psi_m}^{r*}(\mathbf{x}_2, \mathbf{x}_1) - G_{\psi_q \psi_m}^r(\mathbf{x}_2, \mathbf{x}_1) \approx \frac{4\omega^2}{c_P c_{P'} \rho^2} \int_S \int_{S'} G_{\psi_q \psi_0}^r(\mathbf{x}_2, \mathbf{x}) G_{\psi_0 \psi_0}^{r*}(\mathbf{x}', \mathbf{x}) G_{\psi_m \psi_0}^r(\mathbf{x}_1, \mathbf{x}') dS' dS. \quad (16)$$

There is only a single complex conjugate on the right-hand side of eq. (16). Thus, we now have an equation equivalent to the approach of Grechka & Dewangan (2003), containing one cross-correlation and one convolution. Let us use the phases defined earlier to illustrate that the correlation–convolution approach yields the time reverse (complex conjugation) of the correlation–correlation approach. Earlier, we consider the correlation of the PP reflection response ($P1 + P2$), with the PS reflection response ($P1 + S2$): $P1 + P2 - (P1 - S2) = P2 - S2$. This intermediate step is then cross-correlated with the SP reflection response ($S1 + P2$): $P2 - S2 - (S1 + P2) = -(S1 + S2)$. In the correlation–convolution case, the PS reflection response is convolved with the SP reflection response: $P1 + S2 + S1 + P2$. This intermediate step is then cross-correlated with the PP reflection response: $P1 + S2 + S1 + P2 - (P1 + P2) = S1 + S2$. Therefore, we see that the correlation–convolution approach used by Grechka & Dewangan (2003) is equivalent to the complex conjugate of the correlation–correlation approach that we have considered here.

DISCUSSION

Using two different equations derived from the same starting point, we have shown that it is possible to recover the SS reflection response in two different configurations. In the first case, the SS reflection response was recovered by cross-correlating direct S waves with reflected S waves. In this normal configuration for source–receiver interferometry, the SS reflection response between a source and a receiver is recovered (with the correct amplitude-versus-offset behaviour) without having a direct recording of that reflection. In the second case, we showed that the SS reflection response can be recovered, even if we neglect all the terms requiring a shear wave source. In this second case, reflected S waves are cross-correlated with reflected P waves. Thus, the SS response can be recovered using recordings of P and S waves due to P -wave sources only, as shown by Grechka & Tsvankin (2002). The synthetic example illustrates that while the kinematics of this response are correct, the dynamics are not. Using geometrical arguments illustrated in Fig. 5, we have shown that for this second approach to be successful all sources and receivers must be located on the same surface.

Thus, the key differences in eq. (15) from eq. (10) are:

- (1) Source–receiver reciprocity is applied to one of the inputs, requiring that all sources and receivers must be located on the same surface;
- (2) The SS reflection response is recovered despite neglecting the S -wave sources required by theory;
- (3) All direct wave contributions are neglected;
- (4) All sources and receivers must be located on the same surface.

By neglecting the S -wave sources when applying eq. (15), we introduce amplitude errors in Fig. 6(c). For example, since there are no S -wave sources, the PS responses are used, and the PS response tends towards zero amplitude at zero offset (this was also noted by Grechka & Dewangan 2003).

Using the generalized relationship in eq. (8), we can also derive other relationships between P - and S -wave sources and receivers. For example, by following the same steps used to reach eq. (9), but with $Q = 0$, $M = 0$ (P -wave source, P -wave receiver), we can write

$$\begin{aligned} \frac{-4}{\rho^2} \int_S \int_{S'} \partial_j G_{\psi_0 \psi_k}^*(\mathbf{x}_2, \mathbf{x}) \partial_{j'} G_{\psi_k' \psi_k}(\mathbf{x}', \mathbf{x}) G_{\psi_0 \psi_0}^*(\mathbf{x}', \mathbf{x}_1) n_{j'} n_j dS' dS &= G_{\psi_0 \psi_0}(\mathbf{x}_2, \mathbf{x}_1) - G_{\psi_0 \psi_0}^*(\mathbf{x}_2, \mathbf{x}_1) \\ &+ \frac{4}{\rho^2} \int_S \int_{S'} \partial_j G_{\psi_0 \psi_0}^*(\mathbf{x}_2, \mathbf{x}) \partial_{j'} G_{\psi_0' \psi_0}(\mathbf{x}', \mathbf{x}) G_{\psi_0 \psi_0}^*(\mathbf{x}', \mathbf{x}_1) n_{j'} n_j dS' dS \\ &+ \frac{4}{\rho^2} \int_S \int_{S'} \partial_j G_{\psi_0 \psi_k}^*(\mathbf{x}_2, \mathbf{x}) \partial_{j'} G_{\psi_0' \psi_k}(\mathbf{x}', \mathbf{x}) G_{\psi_0 \psi_0}^*(\mathbf{x}', \mathbf{x}_1) n_{j'} n_j dS' dS \\ &+ \frac{4}{\rho^2} \int_S \int_{S'} \partial_j G_{\psi_0 \psi_0}^*(\mathbf{x}_2, \mathbf{x}) \partial_{j'} G_{\psi_k' \psi_0}(\mathbf{x}', \mathbf{x}) G_{\psi_k \psi_0}^*(\mathbf{x}', \mathbf{x}_1) n_{j'} n_j dS' dS. \end{aligned} \quad (17)$$

As in eq. (9), all terms dependent on the SS response have been moved to the left-hand side. Note, with $Q = 0$ and $M = 0$, only one term in the entire equation is dependent on the SS response, and it lies within a surface integral. Eq. (17) could, therefore, be used to

formulate an inverse problem to find $G_{\psi'_k \psi_k}(\mathbf{x}', \mathbf{x})$ given all combinations of PP and PS responses; such an approach is equivalent to applying the multidimensional deconvolution approach to solving interferometric equations (e.g. Wapenaar *et al.* 2008, 2011; van der Neut *et al.* 2011).

In the Introduction, we discussed various methods based on the standard single integral form of interferometry that use P and S waves (or estimates of those) as inputs, for example, the work of Gaiser & Vasconcelos (2010) on seabed data, Bakulin & Mateeva's (2008) work on downhole data, Miyazawa *et al.*'s (2008) work on ambient noise in a downhole setting, the developments of van der Neut *et al.* (2011) in the application of multidimensional deconvolution and the application of Tonegawa & Nishida (2010) to deep earthquake recordings. Thus, we envisage that the representations derived here will find similar applications, but rather than being used to derive new responses between pairs of receivers (or pairs of sources) the new representations explain how new types of wavefields can be derived between existing sources and existing receivers.

Potential applications of the new source–receiver responses are discussed in Curtis & Halliday (2010), for example, in determining source-to-receiver surface wave (or ground-roll noise) estimates, replacing bad or faulty channels in a seismic survey, or as a quality control measure for the results of other forms of seismic interferometry. Furthermore, King & Curtis (2012) show that double-integral source–receiver representations can be used to correct non-physical errors present in the Green's functions estimates from single-integral forms of seismic interferometry when applied, for example, to towed streamer, or other one-sided survey geometries. Poliannikov (2011) show that similar interferometric relations can be used to recover underside reflections using surface sources and receivers, and the internal-multiple prediction method developed by Weglein and co-workers also uses a similar combination of correlations and convolutions (e.g. Weglein *et al.* 1997). With multicomponent recordings allowing the separation of P - and S -wave data, our methods extend existing forms of interferometry to be able to be used with separated P - and S -wavefields.

Also note that the representations derived here are closely related to imaging methods, and therefore allow extension of those imaging methods to P - and S -wave separated wavefields. For example, Halliday & Curtis (2010) show that the imaging method of Oristaglio (1989) is a special case of the acoustic scattering form of source–receiver interferometry, and Vasconcelos *et al.* (2010) link source–receiver interferometry to so-called extended images that are used for localized velocity analysis.

Note from Fig. 5(b) that the intermediate step is equivalent to the difference in traveltimes between the upgoing P and upgoing S legs of the PP and PS reflection responses, respectively. This could be considered as equivalent to a seismological receiver function where transmitted P and S waves are deconvolved to give an event with a traveltimes equivalent to that illustrated in Fig. 5(b) (Galetti & Curtis 2012). Therefore, application of the second step in the $PP + PS = SS$ method could be considered to be equivalent to the correlation of a receiver function with a PS reflection response (or convolution where the complex conjugate form in eq. 16 is used). This observation could lead to a method where an SS response is recovered from transmitted wavefields, or a combination of transmitted wavefields and surface seismic data. Ikelle & Gangi (2007) also discuss the construction of physical events via a non-physical intermediate step. They refer to this intermediate step as a virtual reflection, and show how it can be used to predict internal multiples.

CONCLUSIONS

We have derived generalized source–receiver interferometric integrals for P and S waves, and have shown how these integrals can be used to calculate the SS reflection response between a source and a receiver using wavefields emitted by that source and recorded on other receivers, and wavefields emitted by other sources and recorded only on that receiver. Thus, this SS reflection response can be calculated without directly recording it.

We have shown that the $PP + PS = SS$ method is a special case of these source–receiver integrals, and have identified the key differences between this method and the fully generalized form. These key differences are that the S -wave sources are neglected, source–receiver reciprocity must be applied to one of the inputs of the $PP + PS = SS$ method, and this in turn requires that sources and receivers must be collocated on the same surface. Since this results in singularities where zero offset Green's functions exist, only the reflected (scattered) part of the wavefield is used.

The generalized form includes all components of any source and receiver type, and allows derivation of other new relationships between P - and S -wave source and receivers. For example, we have also shown that the new relationships may be used to formulate an inverse problem to estimate SS responses from PP and PS responses. The new relationships may aid in combining existing P - and S -wave interferometry and imaging methods and source–receiver interferometry and imaging methods to find new applications in acquisition and processing, and in imaging and inversion of P - and S -wave data.

Finally, we noted that the intermediate step of the $PP + PS = SS$ method may be considered as being equivalent to a receiver function, which suggests there may be a possibility of applying a similar technique using transmitted wavefields.

ACKNOWLEDGMENTS

We would like to thank Jeannot Trampert, Vladimir Grechka and an anonymous reviewer for their comments and suggestions which helped to improve the manuscript.

REFERENCES

- Bakulin, A. & Mateeva, A., 2008. Estimating interval shear-wave splitting from multicomponent virtual shear check shots, *Geophysics*, **73**(5), A39–A43.
- Curtis, A. & Halliday, D., 2010. Source-receiver interferometry from unified representation theorems, *Phys. Rev. E*, **81**(4), 046601–1–046601–10.
- Curtis, A. & Robertsson, J.O.A., 2002. Volumetric wavefield recording and near-receiver group velocity estimation for land seismic, *Geophysics*, **67**(5), 1602–1611.
- Curtis, A., Nicolson, H., Halliday, D., Trampert, J. & Baptie, B., 2009. Virtual seismometers in the subsurface of the Earth from seismic interferometry, *Nature Geosci.*, **2**, 700–704, doi:10.1038/NGEO615.
- Gaiser, J.E. & Vasconcelos, I., 2010. Elastic interferometry for ocean bottom cable data: theory and examples, *Geophys. Prospect.*, **58**(3), 347–360.
- Galleti, E. & Curtis, A., 2012. Generalised receiver functions and seismic interferometry, *Tectonophysics*, in press.
- Grechka, V. & Dewangan, P., 2003. Generation and processing of pseudo-shear-wave data: theory and case study, *Geophysics*, **68**(6), 1807–1816.
- Grechka, V. & Tsvankin, I., 2002. PP + PP = SS, *Geophysics*, **67**(6), 1961–1971.
- Halliday, D. & Curtis, A., 2010. An interferometric theory of source-receiver scattering and imaging, *Geophysics*, **75**(6), SA95–SA103.
- Hong, T.-K. & Menke, W., 2006. Tomographic investigation of the wear along the San Jacinto fault, southern California, *Phys. Earth planet. Inter.*, **155**, 236–248.
- Ikelle, L.T. & Gangi, A.F., 2007. Negative bending in seismic reflection associated with time-advanced and time-retarded fields, *Geophys. Prospect.*, **55**, 57–69.
- King, S. & Curtis, A., 2012. Suppressing nonphysical reflections in Green's function estimates using source-receiver interferometry, *Geophysics*, **77**, Q15–Q25.
- van Manen, D.-J., Curtis, A. & Robertsson, J.O.A., 2006. Interferometric modeling of wave propagation in inhomogeneous elastic media using time reversal and reciprocity, *Geophysics*, **71**(4), SI47–SI60.
- Miyazawa, M., Snieder, R. & Venkataraman, A., 2008. Application of seismic interferometry to extract P and S wave propagation and observation of shear wave splitting from noise data at Cold Lake, Canada, *Geophysics*, **73**, D35–D40.
- van der Neut, J., Thorbecke, J., Mehta, K., Slob, E. & Wapenaar, K., 2011. Controlled-source interferometric redatuming by cross-correlation and multi-dimensional deconvolution in elastic media, *Geophysics*, **76**(4), SA63–SA76.
- Oristaglio, M.L., 1989. An inverse scattering formula that uses all the data, *Inverse Probl.*, **5**, 1097–1105.
- Poliannikov, O.V., 2011. Retrieving reflections by source-receiver wavefield interferometry, *Geophysics*, **76**(1), SA1–SA8.
- Robertsson, J.O.A. & Curtis, A., 2002. Wavefield separation using densely deployed, three component, single sensor groups in land surface seismic recordings, *Geophysics*, **67**(5), 1624–1633.
- Robertsson, J.O.A., Blanch, J.O. & Symes, W.W., 1994. Viscoelastic finite-difference modeling, *Geophysics*, **59**, 1444–1456.
- Slob, E., Draganov, D. & Wapenaar, K., 2007. Interferometric electromagnetic Green's functions representations using propagation invariants, *Geophys. J. Int.*, **169**, 60–80.
- Snieder, R., Wapenaar, K. & Larner, K., 2006. Spurious multiples in seismic interferometry of primaries, *Geophysics*, **71**, SI111–SI124.
- Tonegawa, T. & Nishida, K., 2010. Inter-source body wave propagations derived from seismic interferometry, *Geophys. J. Int.*, **183**, 861–868, doi:10.1111/j.1365-246X.2010.04753.x.
- Vasconcelos, I. & Snieder, R., 2008a. Interferometry by deconvolution, Part 1—theory for acoustic waves and numerical examples, *Geophysics*, **73**, S115–S128.
- Vasconcelos, I. & Snieder, R., 2008b. Interferometry by deconvolution: Part 2—Theory for elastic waves and application to drill-bit seismic imaging, *Geophysics*, **73**, S129–S141.
- Vasconcelos, I., Sava, P. & Douma, H., 2010. Nonlinear extended images via image-domain interferometry, *Geophysics*, **75**, 105–115.
- Wapenaar, C.P.A. & Haimé, G.C., 1990. Elastic extrapolation of seismic P- and S-waves, *Geophys. Prospect.*, **38**, 23–60.
- Wapenaar, K., 2003. Synthesis of an inhomogeneous medium from its acoustic transmission response, *Geophysics*, **68**, 1756–1759.
- Wapenaar, K. & Fokkema, J., 2006. Green's function representations for seismic interferometry, *Geophysics*, **71**(4), SI33–SI44.
- Wapenaar, K., van der Neut, J. & Ruigrok, E., 2008. Passive seismic interferometry by multidimensional deconvolution, *Geophysics*, **73**, A51–A56.
- Wapenaar, K., van der Neut, J., Ruigrok, E., Draganov, D., Hunziker, J., Slob, E., Thorbecke, J. & Snieder, R., 2011. Seismic interferometry by crosscorrelation and by multi-dimensional deconvolution: a systematic comparison, *Geophys. J. Int.*, **185**, 1335–1364.
- Weglein, A.B., Gasparotto, F.A., Carvalho, P.M. & Stolt, R.H., 1997. An inverse-scattering series method for attenuating multiples in seismic reflection data, *Geophysics*, **62**, 1975–1989.